In Situ UV Raman Study of the NO_x Trapping and Sulfur Poisoning Behavior of Pt/Ba/γ-Al_2O_3 Catalysts

Dairene Uy,* Kelly A. Wiegand, Ann E. O'Neill, Mark A. Dearth, and Willes H. Weber

Ford Research Laboratory, P.O. Box 2053/MD 3028, Dearborn, Michigan 48121

Received: August 17, 2001; In Final Form: October 26, 2001

In situ Raman experiments excited with 244 nm radiation are carried out on Pt/γ-Al_2O_3 and Pt/Ba/γ-Al_2O_3 catalysts. The addition of Ba allows the normal catalyst to store substantial amounts of NO_x as Ba nitrates under lean burn conditions. Dilute amounts of NO and/or SO_2 plus O_2 in N_2 are flowed over the catalysts, with the temperatures and concentrations chosen to simulate the NO_x trapping and sulfur poisoning characteristics encountered in normal operation. Adsorbed species observed on Pt/γ-Al_2O_3 are nitrite/nitro species and sulfate on γ-Al_2O_3 and NO on Pt. On Pt/Ba/γ-Al_2O_3, in situ UV Raman spectra showed typical NO_x trap behavior: NO_x and SO_x are stored as $Ba(NO_3)_2$ and $BaSO_4$ during lean conditions and released at higher temperatures in H_2 flow. Prolonged SO_2 exposure eventually deactivates the catalyst for NO_x storage. The sulfate purged by heating to 500 °C in H_2 is not completely removed from the catalyst, since it can reappear at lower temperature without additional exposure to SO_2. On both Pt/γ-Al_2O_3 and Pt/Ba/γ-Al_2O_3, NO_x species form more quickly than sulfates under our reaction conditions, but the sulfates are more stable and eventually block NO_x adsorption, since they occupy the same sites.

1. Introduction

Gasoline-powered engines operating near stoichiometry are used in most present-day automobiles. In these engines conventional three-way catalysts (TWCs) are very effective in reducing the emissions of unburned hydrocarbons, CO, and NO_x to levels that comply with the increasingly stringent governmental regulations. Diesel and lean-burn gasoline engines offer a significant fuel economy advantage over stoichiometric gasoline engines, but they have the disadvantage of excessive NO_x emissions that cannot be mitigated by conventional TWCs. Finding a way to reduce NO_x under lean-burn conditions has thus become one of the pressing issues in automotive catalysis. A variety of technologies are currently being investigated for NO_x reduction in both diesel and lean-burn gasoline engines, among which are NO_x traps. These were introduced by Toyota Motor Corporation in the mid-1990s and are composed of a TWC with enhancement of NO_x "storage" behavior.[1,2]

The active components of a NO_x trap are an alkaline earth metal oxide (notably barium oxide) and precious metals (Pt or Pt/Rh) dispersed on γ-Al_2O_3. The engine operates under lean conditions most of time, during which NO_x is stored. It is cycled on a regular basis to slightly rich conditions in order to purge the trap. During lean operation, it is believed that NO is oxidized to NO_2 over the Pt, and subsequently stored as barium nitrate. When the engine is cycled to an air-to-fuel ratio rich of the stoichiometric value, the stored nitrate is reduced to N_2 over the noble metals by H_2, CO, and hydrocarbons in the exhaust, which purges the trap. Since BaO is unstable and transforms into carbonate upon exposure to air, the mechanism may involve the reaction of $BaCO_3$ to $Ba(NO_3)_2$. Finally, while these traps can boast >90% NO_x conversion efficiency at their operating temperature range (300−450 °C), they are highly vulnerable to deactivation by sulfur poisoning. Trace amounts of sulfur in fuel are easily oxidized in the lean exhaust environment and undergo storage as sulfates, which are more stable than nitrates.

While a large number of studies have been performed on NO_x storage and poisoning, a detailed understanding of these mechanisms is still lacking. Fridell and co-workers extensively studied NO_x storage in Pt/BaO/Al_2O_3 and Pt/Rh/BaO/Al_2O_3 systems using FTIR and other methods.[3−5] They observed signatures for several forms of surface nitrates, and they believe atomic oxygen plays a role in the storage of NO_x. Anderson et al. observed both surface and bulk $Ba(NO_3)_2$ and $BaCO_3$[6] using FTIR. Mahzoul et al. presented mechanisms of NO_x storage based on the type of adsorption site on the catalyst,[7] and Kobayashi et al. studied the NO_x trapping cycle using thermodynamic calculations.[8] On the sulfur poisoning side, studies by Matsumoto et al.[9] and Mahzoul et al.[10] show that catalyst deactivation involves the formation of both barium and aluminum sulfates. Meanwhile, Fridell's group[11,12] studied the effects of sulfur poisoning. One mechanism studied was the formation of $BaSO_4$. They also suggested poisoning due to adsorbed sulfur on the precious metal. Both mechanisms inhibit NO_x oxidation and reduction activities of the noble metals. Investigations by Strehlau et al. led to the conclusion that SO_x is preliminarily adsorbed on the BaO surface to form an impenetrable surface layer and that sulfate decomposition occurs via a two-stage mechanism where adsorbed sulfate is first released as SO_2 in reducing conditions, which then reacts with H_2 to form H_2S and H_2O.[13] Finally, Dearth et al. showed that sulfur may be stored in a form other than a sulfate,[14] and Erkfeldt et al. suggested that different forms of sulfur species, deactivating and nondeactivating, are readily adsorbed, desorbed, and transformed into one another on the catalyst.[15,16]

Although UV Raman spectroscopy is extensively used in biological and biochemical studies,[17−19] its employment in catalyst characterization is still fairly uncommon. Li and Stair first demonstrated its utility in the characterization of sulfated

* Author to whom correspondence should be addressed at Ford Motor Company, MD 3028/SRL Building, P.O. Box 2053, Dearborn, MI 48121. Tel: (313) 594-1649. Fax: (313) 322-7044. E-mail: duy@ford.com.

10.1021/jp013191g CCC: $22.00
Published on Web 12/14/2001

zirconia[20] and coke formation in zeolites[21] using 257.2 nm excitation. Li subsequently used the technique to investigate Fe atoms in zeolites,[22] molybdenate species,[23,24] and coke formation.[25] Our group has observed and characterized adsorbed sulfur species on γ-Al_2O_3 and Pt/γ-Al_2O_3 catalysts.[26] Most recently, Stair has constructed a "fluidized bed" technique that tumbles catalyst particles to minimize their thermal degradation and photodecomposition,[27] and used it to study iron peroxo adsorbates on Fe/MFI catalysts.[28] While the possibility of inducing unwanted photochemistry on the sample under investigation exists using UV excitation, the technique offers many advantages over conventional visible Raman spectroscopy: diminished interference from fluorescence, whose Stokes shift is usually much greater than the Raman shifts; enhancement of the signal by the ν^4 factor; possible electronic resonance enhancement, since most catalytic systems absorb in the near UV; and a negligible UV component in the thermal background of a heated catalyst. We have found UV Raman to be particularly valuable for investigating alumina-based catalysts, which tend to fluoresce due to impurities and/or defect states when 633 or 488 nm excitation wavelengths are used. Moreover, alumina itself is transparent for wavelengths longer than ~150 nm, so there is no significant enhancement of its Raman spectrum with 244 nm excitation, nor is there any limitation on the sampling depth due to absorption.

In this work, the NO_x trapping and sulfur poisoning characteristics of Pt/γ-Al_2O_3 and Pt/Ba/γ-Al_2O_3 catalysts are studied using in situ UV Raman spectroscopy, with the objectives of assessing the suitability of this technique for reproducing the trapping behavior and gaining a more detailed mechanistic understanding of the process. The catalysts are heated to varying temperatures under lean and rich gas conditions. Adsorbed nitrates, nitrites, sulfates, and carbonates can be observed in the Raman spectra of the catalysts, confirming observations from previous studies and also yielding new results.

2. Experimental Section

A. Raman Instrumentation. The Raman spectrometer has been described in a previous paper.[26] A commercial Renishaw 1000 Raman microscope equipped with a frequency-doubled argon ion laser for excitation at 244 nm was used, while the microscope employed the usual 180° backscattering geometry. A single-stage spectrometer with a 3600-groove/mm grating dispersed the light, which was detected with a CCD array optimized for UV collection efficiency with a lumogen coating. Grams/32 software from Galactic Industries Corporation controlled the instrument. The laser was focused through a fused-silica window to a 10 μm diameter spot on the catalyst using ~2 mW of laser power. Raman spectra were acquired at the temperatures and gas conditions of interest in either an extended-scan mode, in which the grating was stepped synchronously with the shifting of charge in the CCD array, or in a static scan mode. The exposure time was normally 450 s. Only spectra with Raman shifts longer than 400 cm^{-1} can be obtained, due to the frequency cutoff of the stacked dielectric filters used to attenuate the Rayleigh scattering. Spectra were corrected for the oscillatory transmission characteristics of these filters. The spectrometer was calibrated daily using the single-crystal graphite peak at 1582 cm^{-1} and spectral resolution was ~8 cm^{-1}.

The samples were loaded into a Linkam THMS 600 Stage, which can be heated to 600 °C. Premixed gases at room temperature entered the stage through one side and flowed over the sample. Since we are flowing unheated gases through the Linkam chamber, we would expect the temperature of the catalyst surface to be somewhat lower than the control temperature for the hot stage. This temperature difference is estimated to be ~30 °C at the highest temperatures and flow rates, based on a comparison between the known temperature dependence of the PdO B_{1g} Raman mode and measurements done in the Linkam cell.[29]

B. Catalyst Preparation. The Pt/Ba/γ-Al_2O_3 catalyst was prepared from 0.75 mm diameter γ-Al_2O_3 spheres (Condea Chemie GmbH, Hamburg, Germany) with a surface area of 180 m^2/g (by BET). The spheres were impregnated with 1 wt % Pt as an aqueous solution of hexachloroplatinic acid using the incipient wetness technique. Barium nitrate (aqueous solution) was subsequently added to the platinum-impregnated beads in a second impregnation step to obtain 5 wt % loading. The catalyst was then calcined in air at 500 °C for 1 h. Next, it was conditioned at 600 °C with 5% O_2 in N_2 and 2% H_2:CO (4:1) in N_2 for 30 min each, which removed most of the chloride as HCl. Samples for Raman analysis were then pulverized and were either used directly without further treatment or pretreated in the Raman cell in one of the following ways: (A) exposure to 20% O_2 followed by 5% H_2 for 30 min each at 350 °C, or (B) exposure to 5% H_2 at 500 °C for 30 min. Pretreatment (A) was carried out to be consistent with an XPS study done on the same materials (to be published elsewhere); pretreatment (B) removed the $BaCO_3$. Except for the absence of carbonate in (B), these pretreated samples exhibited the same Raman spectra as the untreated ones.

C. Reaction Conditions. To simulate lean conditions, a gas mixture consisting of 440 ppm NO, 25 ppm SO_2, and 5% O_2 in N_2 was used with a total flow rate of either 50 or 100 sccm at 1 atm. The rich mixture consisted of 5% H_2 in N_2. The lean gas mixture was flowed at 350 °C and the rich at 500 °C. To simplify the experiments, other exhaust gas components such as CO_2, H_2O, and hydrocarbons were excluded from the gas stream. After switching gases we usually waited several minutes before recording spectra. With the cell volume of 33 cm^3 combined with our flow rates, this time was more than adequate to completely exchange the gas. Since the catalyst samples looked very inhomogeneous when viewed under the microscope, multiple spectra were obtained for every gas mixture/temperature condition to ensure that the results were representative.

3. Results

A. Pt/γ-Al_2O_3. To better distinguish the trapping capabilities of the Ba additive, we first studied Pt/γ-Al_2O_3 without Ba. Figures 1 and 3 show spectra of Pt/γ-Al_2O_3 obtained during in situ nitration and sulfation at 350 °C.

Figure 1a shows untreated Pt/γ-Al_2O_3 under N_2 flow. Aside from a broad peak at ~570 cm^{-1} due to the Pt−O stretch of chemisorbed oxygen on Pt[30] and a shoulder at ~800 cm^{-1} due to the alumina,[31] the spectrum of Pt/γ-Al_2O_3 is featureless up to 4000 cm^{-1}. (If the sample is initially treated in H_2 at 500 °C, the chemisorbed oxygen peak disappears.) The small sharp peaks at 1555 and 2330 cm^{-1} arise from gas-phase O_2 and N_2 vibrations, respectively.[32]

Figure 1b shows the spectrum of the catalyst exposed to NO + O_2. Two features appear with this exposure: a peak at 1318 cm^{-1} and a broader band centered in the 1720−1740 cm^{-1} range. The former corresponds to the symmetric N−O stretch of either a nitro (−NO_2) group or a nitrite ion (NO_2^-).[33] The band near ~1720 cm^{-1} is due to the N═O stretch of nitric oxide adsorbed on platinum. NO vibrations have been observed on

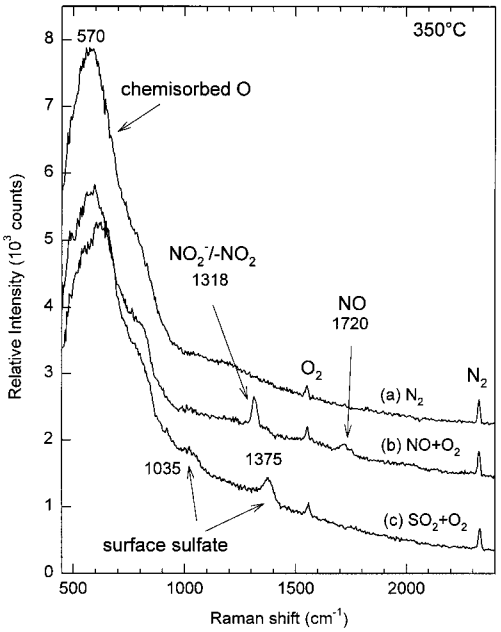

Figure 1. Pt/γ-Al_2O_3 at 350 °C under (a) N_2 flow, (b) NO + O_2 flow, and (c) SO_2 + O_2 flow. Spectra (a) and (b) have been shifted vertically for clarity. Spectrum (a) shows a peak due to chemisorbed oxygen, (b) shows nitrite/nitro species and adsorbed NO, and (c) shows surface sulfates at 1375 and 1035 cm^{-1}.

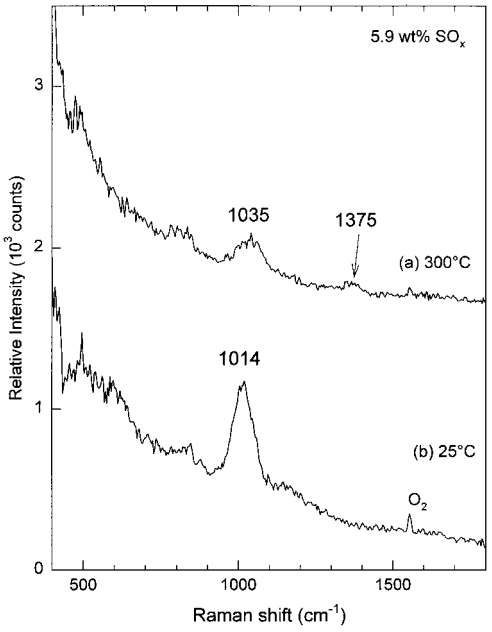

Figure 2. Previously sulfated Pt/γ-Al_2O_3 catalyst with 5.9 wt % SO_x under N_2 flow. Spectrum (a) at 300 °C shows sulfate peaks at 1035 and 1375 cm^{-1}, with the 1035 cm^{-1} peak bigger, in contrast to the sulfate peaks obtained during in situ sulfation. Spectrum (b) obtained at ambient temperature shows only one sulfate peak at 1014 cm^{-1}. Intensities of SO_x species in (a) are different from those of Figure 1(c), suggesting the peaks belong to different SO_x forms.

atop sites on Pt(111) at 1710−1720 cm^{-1},[34,35] on stepped (1780 cm^{-1}) and terrace (1740 cm^{-1}) sites of Pt particles on ZnO,[36] and on Pt on Pt/TiO_2 from ∼1700−1765 cm^{-1}.[37] NO adsorbed on alumina shows bands below 1700 cm^{-1}.[38−40] The spectrum remains unchanged with continued NO + O_2 flow over the next few hours; nitrates are not observed. Switching the gas mixture to pure NO or NO_2 + O_2 gave the same spectrum. These results confirm that at 350 °C Pt/γ-Al_2O_3 by itself is not responsible for trapping NO_x *as a nitrate*.

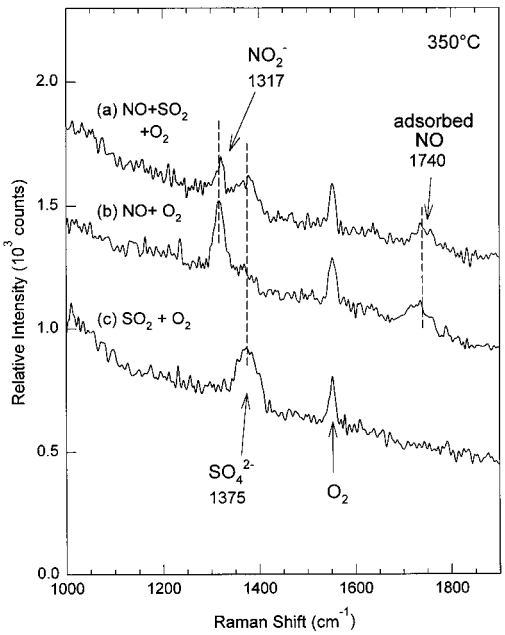

Figure 3. Pt/γ-Al_2O_3 during simultaneous (a) and sequential (b, c) nitration and sulfation. Spectrum (a) shows both SO_x and NO_x species. Removing SO_2 from the gas flow removed the adsorbed SO_x species while the NO_x peaks increased (b). Converting to SO_2 + O_2 flow desorbed the NO_x species and allowed SO_x to reappear (c).

Figure 1c shows the sulfation of a similar Pt/γ-Al_2O_3 sample. Two peaks are visible at 1035 and 1375 cm^{-1}. These have been previously seen in various IR[41] and Raman[42,26] studies of adsorbed SO_x species on γ-Al_2O_3 and Pt/γ-Al_2O_3 and assigned to surface sulfate species on the alumina. The peaks were earlier attributed to a single sulfur species having the structure $(-O-)_3S{=}O$, with the higher frequency band due to the S═O stretch and the lower frequency band due to the S−O stretch.[41,42]

However, our UV Raman data demonstrate that these peaks belong to different species. Figure 1c shows that the 1375 cm^{-1} line is more intense than the 1035 cm^{-1} line. The relative intensity of these bands to one another remained unchanged as the SO_2 and O_2 gas mixture was continuously flowed over the catalyst at 350 °C over the next 1 1/2 hours. These intensities can be compared to those on UV Raman spectra of previously sulfated Pt/γ-Al_2O_3 treated with 800 ppm SO_2 + 10%O_2 at 500 °C for 12 h as discussed in Uy et al.[26] Spectra of this catalyst, which had a 5.9 wt % gain attributed to SO_x, were obtained at 25 °C in air and various temperatures in flowing N_2. The spectrum at 300 °C is shown in Figure 2a. It is similar to the spectrum obtained at 400 °C (not shown) and shows the 1035 cm^{-1} band as more intense than the 1375 cm^{-1} peak. Moreover, the 25 °C spectrum (Figure 2b) shows only a single peak at 1014 cm^{-1}. (The peak exhibits frequency shifts depending on the degree of hydration of the catalyst.[26]) The dependence of the intensity difference between the two peaks on the sulfation conditions suggests that the species corresponding to the 1035 cm^{-1} peak corresponds to a more stable, bulklike form of sulfate, whereas the 1375 cm^{-1} peak is more of a surface complex.

Figure 3a shows the Pt/γ-Al_2O_3 catalyst simultaneously exposed to SO_2 + NO (with O_2) flow. Peaks appear at 1318, 1375, and 1740 cm^{-1}, showing both surface sulfate and NO_x species adsorbed on the catalyst. However, competition for the same adsorption sites exists between the sulfate and NO_x species. NO_x species adsorbed first while the sulfate species appeared several minutes later. When SO_2 was removed from the gas flow, the sulfate peak vanished and the NO_x peaks grew (Figure 3b). Similarly, adsorbed NO_x species vanished and sulfate

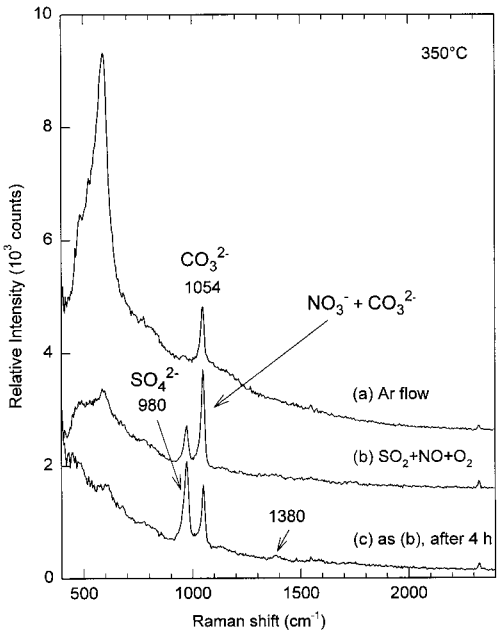

Figure 4. Pt/Ba/γ-Al_2O_3 at 350 °C. Spectrum (a) shows the surface oxygen species near 590 cm^{-1} and the carbonate peak at 1054 cm^{-1}. Spectra (b) and (c) show sulfate and nitrate (plus carbonate) peaks under simultaneous nitration and sulfation. A hint of surface sulfate on the alumina is visible in (c) at 1380 cm^{-1}.

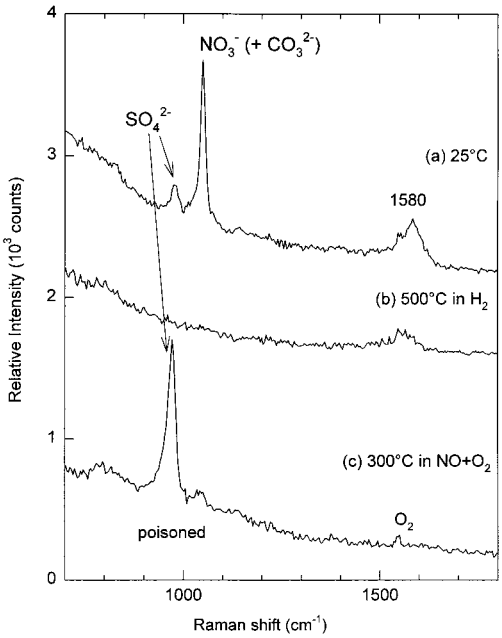

Figure 5. Spectrum (a) shows the catalyst in Figure 4 cooled to 25 °C, showing the same sulfate and nitrate species. The broad peak at 1580 cm^{-1} belongs to a graphitic impurity. Reduction at 500 °C in H_2 removes all traces of the adsorbed species (b), but a sulfur-poisoned catalyst retains the sulfate peak and cannot adsorb NO_x species under NO + O_2 flow (c).

species reappeared when NO was replaced with SO_2 (Figure 3c). Alternating SO_2 and NO flow resulted in seeing either sulfate or NO_x species adsorbed onto the catalyst. Eventually, however, the NO_x species cannot displace the sulfate species. These results show that NO reacts more quickly, but the adsorbed sulfates formed from SO_2 are more stable under our gas conditions.

B. Pt/Ba/γ-Al_2O_3. *Simultaneous Sulfation and Nitration.* Figure 4 shows spectra of untreated Pt/Ba/γ-Al_2O_3 at 350 °C. The top trace (a) shows the spectrum obtained in argon gas before sulfation and nitration. A strong peak at 1054 cm^{-1} is initially observed, which is due to the ν_1 symmetric C−O stretch of carbonate in $BaCO_3$.[33] The BaO formed after sample calcination is unstable in air and has been transformed to $BaCO_3$, which we observe in this figure. Reducing the sample at 500 °C in H_2 removes the peak.

Figures 4b and 4c show the catalyst simultaneously exposed to SO_2 and NO (with O_2). Two strong peaks are visible at 1054 and 980 cm^{-1}. The latter is due to the prominent ν_1 symmetric S−O stretch of SO_4^{2-} in $BaSO_4$.[33] The 1054 cm^{-1} peak is attributed to both the ν_1 symmetric (C−O, N−O) stretch of the free carbonate and nitrate of barium.[33,43] The frequency of the carbonate peak is actually ∼10 cm^{-1} higher than the corresponding nitrate peak in the bulk barium compound at room temperature. However, as observed on this catalyst using UV Raman, the nitrate and carbonate overlap. Although the peaks are not resolvable, we know that the carbonate is transformed to nitrate with NO in the gas stream from the chemistry. Moreover, the shrinking core model proposed by Hepburn et al. describes a core of $BaCO_3$ being progressively transformed to $Ba(NO_3)_2$ upon nitration,[44] and barium carbonates have been observed by FTIR[7] and XRD[45] to decompose upon nitration. Figure 4c shows the sample 4 h later; the spectrum is unchanged except for an additional weak feature at 1380 cm^{-1} due to surface sulfate formation on the alumina. Although the SO_2 concentration in the gas stream is ∼18× lower than the NO concentration, the sulfate and nitrate/carbonate peaks have comparable intensities. The increase in the sulfate peak and decrease in the nitrate/carbonate peak should not be taken as absolute, since taking a spectrum of a different area of the catalyst can show reversed intensities. (This highlights a difficulty in doing Raman microscopy of an inhomogeneous sample.) Last, the very large peak at 590 cm^{-1} in Figure 4a seems to be due to some form of surface oxide or adsorbed oxygen species, since it forms only under oxidizing gas conditions and is removed at higher temperatures with H_2.

Figure 5a shows a spectrum of the catalyst in air after cooling to 25 °C. The sulfates and nitrates formed at 350 °C remain on the catalyst. The broad peak at 1580 cm^{-1} is due to the C═C stretch of sp^2 bonded graphitic carbon[46] or an olefinic stretch of other carbonaceous impurity.[47] It is occasionally observed in our samples, especially in the presence of H_2 gas.

The catalyst is regenerated by heating to 500 °C in H_2. Adsorbed sulfates and nitrates are removed as shown in Figure 5b. (The nitrate fully decomposes at lower temperature.) However, this reduction treatment is insufficient to remove all traces of sulfur, if the catalyst has been subjected to repeated and prolonged exposure to SO_2. Although the sulfate peak disappears at 500 °C, it reappears when the catalyst is cooled to 350 °C. In this state nitrate can no longer be adsorbed; the sulfur has poisoned the NO_x trapping ability of the catalyst. This is depicted in Figure 5c, where flowing NO + O_2 does not result in adsorbed nitrate.

Sulfation. Figure 6a shows the behavior of (unreduced) catalyst exposed to SO_2 and O_2 at 350 °C. The top spectrum shows the catalyst before SO_2 exposure with the carbonate peak at 1054 cm^{-1}. The bottom spectrum shows the catalyst in SO_2 flow, with adsorbed sulfate at 980 cm^{-1}. The simultaneous presence of both peaks in the bottom spectrum indicates that either sulfate formation did not consume all of the carbonate or that only a fraction of the barium sites were initially occupied with carbonate.

Nitration. Figure 6b shows Pt/Ba/γ-Al_2O_3 during nitration. At 350 °C, the spectrum (top trace) shows only a single nitrate

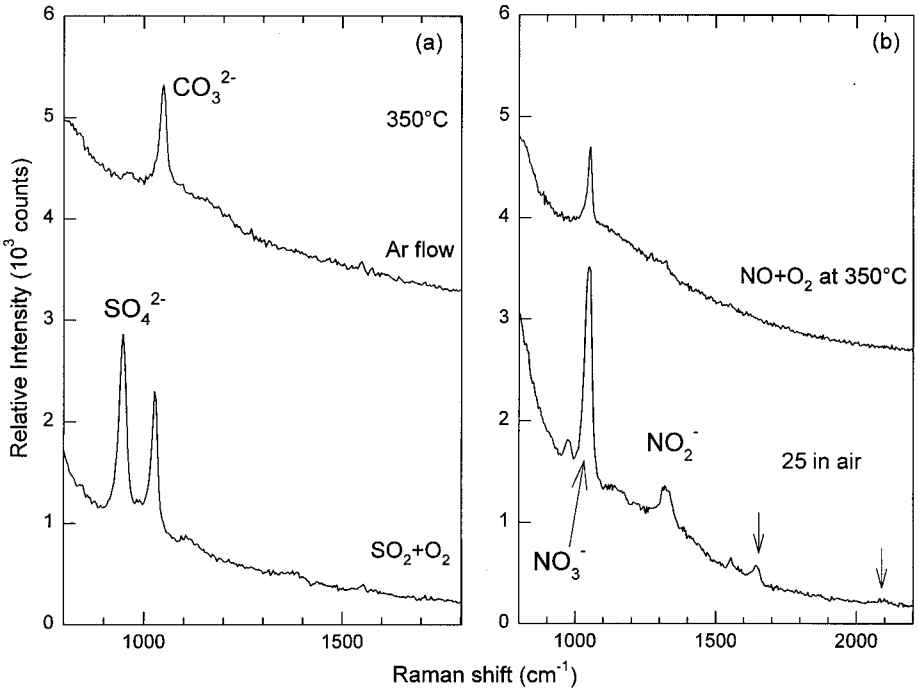

Figure 6. Sulfation (a) and nitration (b) of Pt/Ba/γ-Al_2O_3. Spectrum (a) shows barium sulfate formation without completely displacing the carbonate. Spectrum (b) shows the formation of both nitrate and nitrite species at 25 °C, in contrast to a simultaneous sulfation and nitration (Figure 5a). The arrows point to additional (bulk) nitrate peaks. The small peak at ~980 cm^{-1} is due to defective BaO.

peak at 1054 cm^{-1} whether the sample had been previously reduced, exposed to $NO_2 + O_2$, or had 4% H_2O added to the gas mixture. However, the spectrum also shows a strong nitrite/nitro species peak at 1323 cm^{-1} upon cooling to room temperature. The other peaks visible at 1642 cm^{-1} ($2\nu_2$) and 2094 cm^{-1} ($2\nu_1$) belong to barium nitrate.[48] Note that the sample that was simultaneously sulfated and nitrated did not show nitrite/nitro species at 25 °C (Figure 5a). The results here support the results obtained for Pt/γ-Al_2O_3 catalysts, i.e., the nitrite and sulfate adsorb on the same sites, with sulfate being the more strongly held species. (The small peak at ~ 980 cm^{-1}(in the bottom trace of Figure 6b) is not due to sulfate but to defect-rich BaO.[49])

4. Discussion

A. Pt/γ-Al_2O_3. The exposure of Pt/γ-Al_2O_3 to $NO + O_2$ does not lead to nitrate (D_{3h} symmetry) formation on the catalyst at 350 °C. This agrees with studies concluding that a basic element is necessary to trap NO_x as nitrates for later reduction.[50,51] The Raman signatures of the nitrite/nitro species and adsorbed nitric oxide were generally either much weaker than the bands associated with adsorbed species on the Pt/Ba/γ-Al_2O_3 catalysts or are absent on some in situ runs. Moreover, adsorbed NO_x species on γ-Al_2O_3 are weakly bound; 500 sccm of flowing N_2 easily removes them even at 25 °C (where they are more stable than at higher temperatures).[30]

When the Pt/γ-Al_2O_3 is *cooled to room temperature* in the presence of $NO + O_2$, a small amount of aluminum nitrate is formed. Several small new peaks appear at 998, 1037, 1287, and 1583 cm^{-1}, which exactly match those observed in Raman spectra of bulk *dehydrated* aluminum nitrate. The peaks at 1287 and 1583 cm^{-1} also match the FTIR bands observed by Westerberg and Fridell for monodentate nitrate species on Al_2O_3 at elevated temperatures.[5]

The spectra of in situ sulfated (Figure 1c) and previously sulfated Pt/γ-Al_2O_3 (Figure 2) at elevated temperatures, showing different intensities of the 1035 and 1380 cm^{-1} SO_x species depending on treatment, clearly indicate that two forms of SO_x exist on alumina. A study using isotopic substitution concluded that both peaks belonged to only one species,[41] with the peak at 1380 cm^{-1} appearing only when the alumina was well dehydroxylated.[52] However, this does not fully account for the different intensities of the two SO_x peaks we have observed. Furthermore, the lower frequency peak at 1035 cm^{-1} which we attributed to a more bulklike species is less than 150 cm^{-1} away from the symmetric S−O stretching mode of SO_4^{2-} in bulk dehydrated crystalline (1127 cm^{-1}) or hydrated crystalline and aqueous sulfates (983 cm^{-1}).[26,33]

The simultaneous exposure of Pt/γ-Al_2O_3 to SO_2 and NO in O_2 shows that the nitrite/nitro and surface sulfate species compete for the same sites on the alumina and that the former have a higher formation rate. Analogous results are obtained for Pt/Ba/γ-Al_2O_3, as discussed below.

B. Pt/Ba/γ-Al_2O_3. Our observations on Pt/Ba/γ-Al_2O_3 catalysts show the existence of sulfates, nitrates, and carbonates of barium during lean conditions, which disappear under rich conditions. Only one type of nitrate species is observed, which most probably corresponds to a more bulklike form of barium nitrate than a surface nitrate. Bulklike barium nitrate has been previously observed,[6,7] although only surface species were observed in another study.[5] Our spectra also showed that (noncrystalline) barium carbonates are not completely decomposed upon the formation of barium sulfate. This is different from observations of other workers who see carbonate peaks disappear upon sulfation (and nitration).[9,10] Their observations coupled with ours of only a single type of adsorbed nitrate species suggests that our sensitivity may be partly limited to observing species that are present in larger quantities or in more bulklike form on the catalyst, unless their vibrations are resonantly enhanced.

Our spectra also showed that sulfate deposits on the Pt/Ba/γ-Al_2O_3 catalyst can migrate or diffuse through the washcoat. This was demonstrated when the Raman signature for the sulfate at 983 cm^{-1} disappeared at 500 °C in H_2 flow and reappeared

when the catalyst was cooled to 350 °C in the same gas flow (H_2). The fact that the sulfate was reduced at 500 °C indicates that the barium sulfate particles formed are still very small, since bigger particles are more difficult to reduce.[50] Elemental sulfur[53] or PtS[54,55] may also have been formed during the reduction process, but the reappearance of the sulfate peak without O_2 in the gas flow is more puzzling. Possibly the reduced S can reoxidize by reacting with the support at lower temperature to yield sulfate.

The simultaneous sulfation and nitration of the Pt/Ba/γ-Al_2O_3 catalyst at 350 °C showed the existence of *nitrates* (and sulfates), in contrast to the Pt/γ-Al_2O_3 samples, which showed *nitrites* (or nitro species) and not nitrates. At 350 °C, it appears that whatever nitrites are formed are quickly trapped as nitrates of barium and thus no trace of nitrites remain on the Pt/Ba/γ-Al_2O_3. The formation of nitrites as a prerequisite for nitrate formation has also been suggested by Westerberg and Fridell.[5] However, when the Pt/Ba/γ-Al_2O_3 catalyst is cooled to room temperature, exposure to NO + O_2 showed both nitrates and nitrites. We can make two conclusions from this observation. The first and more likely one is that the nitrites formed on the alumina, and not on the barium. This can be deduced from the results of the nitration of Pt/γ-Al_2O_3 in this work and elsewhere[30] (and unpublished results). At 350 °C, a small amount of nitrite formed on the alumina, while large amounts of nitrate and nitrite formed at room temperature in the presence of NO + O_2 or NO_2. The absence of nitrite at 25 °C on the Pt/Ba/γ-Al_2O_3 catalyst after simultaneous sulfation and nitration is also reminiscent of the competition between nitrite and sulfate for the same sites on the Pt/γ-Al_2O_3 catalyst. A second conclusion is that a step in the sulfur poisoning of the Pt/Ba/γ-Al_2O_3 catalysts may be the blocking of sites that form nitrites, which are subsequently transformed to nitrates. The presence of nitrite at room temperature may be due to the slowness of the nitrite to form the nitrate at 25 °C (water may be the mediator in this process), or the reactive sites do not have the turnover frequency to populate the nitrate storage sites. Adsorbed nitrates are not displaced by SO_2 on Ba-containing catalysts.[10]

We have also seen that SO_2 in the gas stream initially *increases* nitrate formation on Pt/Ba/γ-Al_2O_3. The intensity of the adsorbed nitrate peak is larger on the reduced (i.e. no carbonate) catalyst when SO_2 is included in the gas flow. It is well-known that oxides of S and N have a complex chemistry depending on reaction conditions;[56] SO_x and NO_x may thus directly react with one another to increase nitrate formation. Our other studies, using a lab pulsating combustor flow reactor, also show an increase in NO_x storage efficiency for traps when sulfur poisoning is initiated, but the poisoning soon diminishes trap capacity and efficiency declines. A similar effect has been observed by Wilde and Marin on Na-γ-alumina, where adsorption of NO + O_2 was enhanced by SO_2 in the gas stream.[57]

It was shown in Section 3 that nitrites adsorbed more quickly than sulfates on Pt/γ-Al_2O_3 under our reaction conditions. Comparable behavior is observed for nitrates and sulfates on the Pt/Ba/γ-Al_2O_3 catalysts. Figure 7 monitors the growth of these species by a series of spectra taken at 60-s intervals, starting at the top, with exposure times of 60 s. The prereduced catalyst is exposed to SO_2 + O_2 in Figure 7a, and to NO + O_2 in Figure 7b at 350 °C. The spectra show that the sulfate species takes a few minutes to appear while the nitrate peak can be observed immediately.

While nitrate formation involving the reaction of atomic oxygen with NO or NO_2 has been proposed,[4] atomic O has not previously been directly observed on Pt/Ba/γ-Al_2O_3. Figure 7 shows the growth of a peak near 590 cm^{-1} that we have attributed to a surface oxide or adsorbed atomic oxygen species. The peak grows in an O_2 environment and is removed in a rich one, but its specific role in NO_x and SO_x trapping is yet to be fully elucidated.

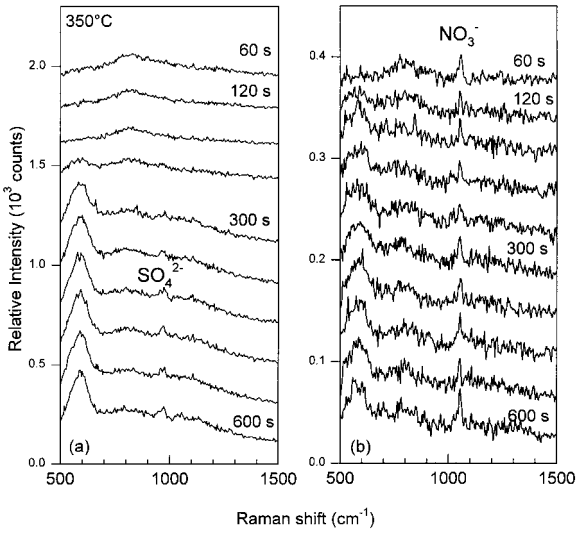

Figure 7. Sulfation (a) and nitration (b) of Pt/Ba/γ-Al_2O_3 at 350 °C. Raman spectra with 60 s exposure times were obtained every 60 s, beginning at the top. All except the bottom spectra are displaced for clarity. Whereas the appearance of the nitrate peak in the first trace shows almost immediate adsorption of NO, the sulfate peak takes several minutes to form.

Finally, we have observed the formation of bulk $BaCO_3$ crystals during the in situ experiments. Raman spectra showed very strong peaks at 686, 1054, 1395, 1500, 1709, 1755 cm^{-1} which are characteristic of barium carbonate (Figure 8). These micron-sized crystals appeared white and glittery under the microscope and are purposely avoided when recording spectra. However, they cannot be completely removed under our conditions, since they melt at temperatures over 900 °C. The barium carbonates initially observed in the sample may have sintered to form bulk crystals. These crystals may also be responsible for the carbonate signal that persists in the presence of sulfate in Figure 6a.

C. Possible Photoeffects of UV for Raman Excitation. One possible concern in Raman spectroscopy experiments is the heating of the sample due to the high laser power concentrated on a small sample spot. Using a UV laser as an excitation source compounds the problem as the possibility for photochemistry or photodegradation of the sample or adsorbed species exists as well. In this section, we discuss the possibility that our observations are influenced by 244 nm excitation.

The use of hydrocarbons in the reducing phase has been purposely avoided in this study since the UV photodecomposes most organic compounds. Along with a black spot that appears on the sample where the laser has been focused, a peak at ~1580 cm^{-1} forms, which can grow rapidly during sequential spectral accumulations to indicate the increasing formation of coke species under UV exposure.

The carbonates, nitrates, and sulfates seen on the Pt/Ba/γ-Al_2O_3 catalysts are little affected by the UV excitation. To validate this, we obtained sequential spectra similar to Figure 7 under static gas and temperature conditions. Generally, these species are stable under UV excitation when the corresponding gases (NO/NO_2, CO_2, and SO_2 with O_2) are flowed over the surface of the catalyst. Carbonates and sulfates are stable in N_2 or air and may decrease very slightly under H_2 at 350 °C. Nitrate

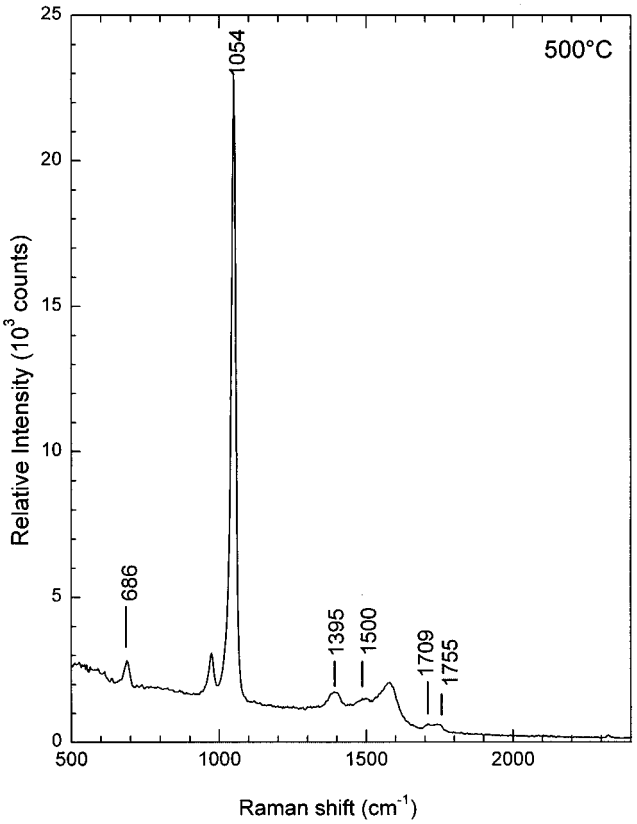

Figure 8. Raman spectrum of crystalline $BaCO_3$ which has formed during the in situ experiments. The labeled peaks all belong to $BaCO_3$. Note that the symmetric stretching C−O peak at 1054 cm^{-1} is ∼20× larger than the initial carbonate species observed, shown in Figures 4a and 6a.

peaks diminish slightly in air or N_2. While stable crystalline nitrates that are irradiated with UV light are known to produce the nitrite[58] and peroxonitrite ($ONOO^-$) ions,[59] surface nitrate species do *not* do so.[60] We have indeed seen strong nitrite peaks in UV Raman spectra of bulk crystalline nitrates, which are very small or absent when HeNe excitation is used. Aside from photoinduced nitrite formation, the intensities of the observed nitrites may also be enhanced. In any case, photoinduced nitrite formation does not occur on our catalyst samples under UV excitation. However, NO adsorbed in on-top sites on Pt, which gives the band we observe at 1720−1740 cm^{-1}, can be photodesorbed by 244 nm radiation.[61,62] Also, NO_2 on Pt may be photodissociated by 244 nm light, since this is known to happen with NO_2 in the gas phase[63] and adsorbed on Pd(111).[64] These processes may kinetically limit the adsorption of NO and its subsequent transformation into nitrate on the catalyst.

5. Summary and Conclusions

We have observed the NO_x trapping and sulfur poisoning behavior of Pt/γ-Al_2O_3 and Pt/Ba/γ-Al_2O_3 catalysts using in situ UV Raman spectroscopy. On the Pt/Ba/γ-Al_2O_3 catalysts, UV Raman successfully reproduces the results observed by other workers. The catalyst stores NO_x as barium nitrates at lean operating conditions, which are released when conditions are switched to rich. Moreover, sulfate formation competes with nitrate adsorption when SO_2 is a constituent of the gas mixture, resulting in the deactivation of the catalyst by the more stable sulfate. Both barium sulfate and a surface sulfate on the alumina were observed on the Pt/Ba/γ-Al_2O_3 catalyst. Also, crystalline $BaCO_3$ was observed to form after continuous "operation" of the catalyst.

We have also made a number of observations regarding adsorption of SO_x and NO_x on the Pt/γ-Al_2O_3 and Pt/Ba/γ-Al_2O_3 catalysts that are unique to this work:

1. Adsorbed nitrite/nitro species and NO have been observed on Pt/γ-Al_2O_3, which are formed more rapidly than sulfates under simultaneous exposure to NO and SO_2 with O_2. Alternating between NO and SO_2 flow shows NO_x and SO_x species being alternately adsorbed on the catalyst, suggesting they dislodge each other to occupy the same sites. Eventually, the greater stability of the sulfate prevents it from being desorbed by the NO_x.

2. Surface sulfate formed on the Pt/γ-Al_2O_3 catalysts, with frequencies at 1035 and 1375 cm^{-1}, belong to two different species. In situ sulfation at 350 °C shows the 1375 peak to be stronger, while spectra of previously sulfated Pt/γ-Al_2O_3 with 5.9 wt % SO_x taken at 300 °C show the 1035 cm^{-1} peak to be larger. The proximity of the latter peak to the prominent symmetric S−O stretch of bulk or aqueous sulfates (∼1000 cm^{-1}) suggests this species may be more bulklike.

3. Nitrite (or nitro) species along with nitrates formed on the Pt/Ba/γ-Al_2O_3 catalyst after nitration at 350 °C and cooling to room temperature. This contrasts with a catalyst that has been simultaneously sulfated and nitrated, which showed nitrates as the only NO_x species at 25 °C. We conclude that either the nitrites formed exclusively on the alumina, or that a step in the sulfur poisoning of the Pt/Ba/γ-Al_2O_3 may be the blocking of sites for nitrite formation by the sulfate.

4. The adsorption of NO_x is initially boosted by the presence of SO_2 in the gas stream. Nitrates are also adsorbed faster than sulfates on Pt/Ba/γ-Al_2O_3 under our reaction conditions.

5. The sulfate peak on the Pt/Ba/γ-Al_2O_3 catalyst disappears during reduction at 500 °C in H_2. Its reappearance after cooling to 350 °C in H_2 suggests that the reduced S can react with O from the support.

Acknowledgment. We thank George W. Graham for helpful discussions and Ben D. Poindexter for assistance in setting up the gas flow system.

References and Notes

(1) Miyoshi, N.; Matsumoto, S.; Katoh, K.; Tanaka, T.; Harada, J.; Takahashi, N.; Yokota, K.; Sugiura, M.; Kasahara, K. *SAE Paper 950809*, 1995.

(2) Miyoshi, N.; Matsumoto, S. *Sci. Technol. Catal.* **1998**, 245.

(3) Fridell, E.; Skoglundh, M.; Johansson, S.; Westerberg, B.; Törncrona, A.; Smedler, G. Investigations of NO_x storage catalysts. In *Catalysis and Automotive Pollution Control IV*; Kruse, N., Frennet, A., Bastin, J.-M., Eds.; Elsevier Science B. V.: Amsterdam, 1998; Vol. 116, pp 537−547.

(4) Fridell, E.; Skoglundh, M.; Westerberg, B.; Johansson, S.; Smedler, G. *J. Catal.* **1999**, *183*, 196.

(5) Westerberg, B.; Fridell, E. *J. Mol. Catal. A* **2001**, *165*, 249.

(6) Anderson, J. A.; Paterson, A. J.; Fernández-Garcia, M. NO_x storage and reduction over Pt/Ba/Al_2O_3. In *12th International Congress on Catalysis*; Corma, A., Melo, F. V., Mendioroz, S., Fierro, J. L. G., Eds.; Elsevier Science B. V.: Amsterdam, 2000; Vol. 130, pp 1331−1336.

(7) Mahzoul, H.; Brilhac, J. F.; Gilot, P. *Appl. Catal. B* **1999**, *20*, 47.

(8) Kobayashi, T.; Yamada, T.; Kayano, K. *SAE Paper 970745*, 1997.

(9) Matsumoto, S.; Ikeda, Y.; Suzuki, H.; Ogai, M.; Miyoshi, N. *Appl. Catal. B* **2000**, *25*, 115.

(10) Mahzoul, H.; Limousy, L.; Brilhac, J. F.; Gilot, P. *J. Anal. Appl. Pyrolysis* **2000**, *56*, 179.

(11) Amberntsson, A.; Westerberg, B.; Engström, P.; Fridell, E.; Skoglundh, M. Sulphur dioxide deactivation of NO_x storage catalysts. In *Catalyst Deactivation*; Delmon, B., Froment, G. F., Eds.; Elsevier Science B. V.: Amsterdam, 1999; Vol. 126, pp 317−324.

(12) Engström, P.; Amberntsson, A.; Skoglundh, M.; Fridell, E.; Smedler, G. *Appl. Catal. B* **1999**, *22*, L241.

(13) Strehlau, W.; Kreuzer, T.; Leyrer, J.; Hori, M.; Lox, E. S.; Hoffman, M. *SAE Paper 962047*, 1996.

(14) Dearth, M. A.; Hepburn, J. S.; Thanasiu, E.; McKenzie, J.; Horne, G. S. *SAE Paper 982595*, 1998.
(15) Erkfeldt, S.; Larsson, M.; Hedblom, H.; Skoglundh, M. *SAE Paper 1999-01-3504*, 1999.
(16) Erkfeldt, S.; Skoglundh, M.; Larsson, M. Poisoning and regeneration of NO_x adsorbing catalysts for automotive applications. In *Catalyst Deactivation*; Delmon, B., Froment, G. F., Eds.; Elsevier Science B. V.: Amsterdam, 1999; Vol. 126, pp 211−218.
(17) Sokolov, L.; Mukerji, I. *J. Phys. Chem. B* **2000**, *104*, 10835.
(18) Aki, M.; Ogura, T.; Shinzawa-Itoh, K.; Yoshikawa, S.; Kitagawa, T. *J. Phys. Chem. B* **2000**, *104*, 10765.
(19) Asher, S. A. *Anal. Chem.* **1993**, *65*, 201.
(20) Li, C.; Stair, P. C. *Catal. Lett.* **1996**, *36*, 119.
(21) Li, C.; Stair, P. C. *Catal. Today* **1997**, *33*, 353.
(22) Yu, Y.; Xiong, G.; Li, C.; Xiao, F.-S. *J. Catal.* **2000**, *194*, 487.
(23) Hu, Y.; Dong, L.; Wang, J.; Chen, Y.; Li, C.; Li, M.; Feng, Z.; Ying, P. *Chem. Lett.* **2000**, *8*, 904.
(24) Xiong, G.; Feng, Z.; Li, J.; Yang, Q.; Ying, P.; Xin, Q.; Li, C. *J. Phys. Chem. B* **2000**, *104*, 3581.
(25) Li, J.; Xiong, G.; Feng, Z.; Liu, Z.; Xin, Q.; Li, C. *Microporous Mesoporous Mater.* **2000**, *39*, 275.
(26) Uy, D.; Dubkov, A.; Graham, G. W.; Weber, W. H. *Catal. Lett.* **2000**, *68*, 25.
(27) Chua, Y. T.; Stair, P. C. *J. Catal.* **2000**, *196*, 66.
(28) Gao, Z.-X.; Kim, H.-S.; Stair, P. C.; Sachtler, W. M. H. *J. Phys. Chem. B* **2001**, *102*, 6186.
(29) McBride, J. R. Raman and optical studies of the oxides of Pd and Pt. Doctoral thesis, University of Michigan, 1992.
(30) Uy, D.; O'Neill, A. E.; Weber, W. H. *Appl. Catal. B* **2002**, *35*, 219.
(31) Deo, G.; Hardcastle, F. D.; Richards, M.; Hirt, A. M.; Wachs, I. E. In *Novel Materials in Heterogeneous Catalysis*; Baker, R. T. K., Murrell, L. L., Eds.; American Chemical Society: Washington, DC, 1990; Vol. 437, p 317.
(32) Herzberg, G. *Infrared and Raman Spectra*; Van Nostrand Reinhold: New York, 1979.
(33) Nakamoto, K. *Infrared and Raman Spectra of Inorganic and Coordination Compounds. Part A. Theory and Applications in Inorganic Chemistry*, 5th ed.; John Wiley & Sons: New York, 1997.
(34) Agrawal, V. K.; Trenary, M. *Surf. Sci.* **1991**, *259*, 116.
(35) Gland, J. L.; Sexton, B. A. *Surf. Sci.* **1980**, *94*, 355.
(36) Boccuzzi, F.; Guglielminotti, E. *Surf. Sci.* **1992**, *271*, 149.
(37) Fang, S. M.; White, J. M. *J. Catal.* **1983**, *83*, 1.
(38) Keiski, R. L.; Härkönen, M.; Lahti, A.; Maunula, T.; Savimäki, A.; Slotte, T. An infrared study of CO and NO adsorption on Pt, Rh, Pd 3-way catalysts. In *Catalysis and Automotive Pollution Control III*; Frennet, A., Bastin, J.-M., Eds.; Elsevier Science B. V.: Amsterdam, 1995; Vol. 96, pp 85−96.
(39) Terenin, A.; Roev, L. *Spectrochim. Acta* **1959**, *15*, 274.
(40) Terenin, A.; Roev, L. *Spectrochim. Acta* **1959**, *15*, 946.
(41) Saur, O.; Bensitel, M.; Mohammed Saad, A. B.; Lavalley, J. C.; Tripp, C. P.; Morrow, B. A. *J. Catal.* **1981**, *99*, 104.
(42) Spielbauer, D. *Appl. Spectrosc.* **1995**, *49*, 650.
(43) Xie, S.; Mestl, G.; Rosynek, M. P.; Lunsford, J. H. *J. Am. Chem. Soc.* **1997**, *119*, 10186.
(44) Hepburn, J. S.; Kenney, T.; McKenzie, J.; Thanasiu, E.; Dearth, M. A. *SAE Paper 982595*, 1998.
(45) Balcon, S.; Potvin, C.; Salin, L.; Tempère, J. F.; Djèga-Mariadassou, G. *Catal. Lett.* **1999**, *60*, 39.
(46) Dresselhaus, M. S.; Pimenta, M. A.; Eklund, P. C.; Dresselhaus, G. Raman scattering in fullerenes and related carbon-based materials. In *Raman Scattering in Materials Science*; Weber, W. H., Merlin, R., Eds.; Springer-Verlag: Berlin, 2000; pp 314−364.
(47) Dollish, F. R.; Fateley, W. G.; Bentley, F. F. *Characteristic Raman Frequencies of Organic Compounds*; John Wiley & Sons: New York, 1974.
(48) Waterland, M. R.; Myers Kelley, A. *J. Chem. Phys.* **2000**, *113*, 6760.
(49) Mestl, G.; Rosynek, M. P.; Lunsford, J. H. *J. Phys. Chem. B* **1997**, *101*, 9321.
(50) Takahashi, N.; Shinjoh, H.; Iijima, T.; Suzuki, T.; Yamazaki, K.; Yokota, K.; Suzuki, H.; Miyoshi, N.; Matsumoto, S.; Tanizawa, T.; Tanaka, T.; Tateishi, S.; Kasahara, K. *Catal. Today* **1996**, *27*, 63.
(51) Yamazaki, K.; Suzuki, T.; Takahashi, N.; Yokota, K.; Sugiura, M. *Appl. Catal. B* **2001**, *30*, 459.
(52) Pieplu, A.; Saur, O.; Lavalley, J. C.; Pijolat, M.; Legendre, O. *J. Catal.* **1996**, *159*, 394.
(53) Mohammed Saad, A. B.; Saur, O.; Wang, Y.; Tripp, C. P.; Morrow, B. A.; Lavalley, J. C. *J. Phys. Chem.* **1995**, *99*, 4620.
(54) Melchor, A.; Garbowski, E.; Mathieu, M. V.; Primet, M. *React. Kinet. Catal. Lett.* **1985**, *29*, 371.
(55) Wang, T.; Vazquez, A.; Kato, A.; Schmidt, L. D. *J. Catal.* **1982**, *78*, 306.
(56) Greenwood, N. N.; Earnshaw, A. *Chemistry of the Elements*; Pergamon Press: Oxford, 1984.
(57) De Wilde, J.; Marin, G. B. *Catal. Today* **2000**, *62*, 319.
(58) Narayanswamy, L. K. *Trans. Faraday Soc.* **1935**, *31*, 1411.
(59) Plumb, R. C.; Edwards, J. O. *J. Phys. Chem.* **1992**, *96*, 3245.
(60) Vogt, R.; Finlayson-Pitts, B. J. *J. Phys. Chem.* **1995**, *99*, 17269.
(61) Mieher, W. D.; Pelak, R. A.; Ho, W. *Surf. Sci.* **1996**, *359*, 23.
(62) Fukutani, K.; Murata, Y. *Surf. Sci.* **1997**, *390*.
(63) Okabe, H. *Photochemistry of Small Molecules*; John Wiley & Sons: New York, 1978.
(64) Hasselbrink, E.; Jakubith, S.; Nettesheim, S.; Wolf, M.; Cassuto, A.; Ertl, G. *J. Chem. Phys.* **1990**, *92*, 3154.